Journal of Building Engineering 91 (2024) 109525

Contents lists available at ScienceDirect

Journal of Building Engineering

journal homepage: www.elsevier.com/locate/jobe

Impact of sound-insulated joints in the dynamic behavior of Cross-Laminated Timber structures

Matteo Salvalaggio [a,*,1], Filippo Lorenzoni [b], Maria Rosa Valluzzi [a]

[a] DBC – Department of Cultural Heritage, University of Padova, Piazza Capitaniato 7, 35139, Padova, Italy
[b] Department of Geosciences, University of Padova, Via G. Gradenigo 6, 35131, Padova, Italy

ARTICLE INFO

Keywords:
Cross laminated timber CLT
Operational modal analysis OMA
Structural dynamics
Acoustic insulation
Finite element FE

ABSTRACT

Cross-Laminated Timber (CLT) has gained an increasing success and widespread diffusion among wood products. Due to the novelty of the components and the dry-assembling techniques, certain aspects of its behavior and performance remain unexplored; among these, the use of sound-insulated joints and brackets, along with their possible drawbacks on mechanical performance.

In this paper the authors discuss the results of dynamic identification (ID) tests carried out on twin full-size CLT mockups (two-story), one of which was furnished with sound-insulation details based on an elastomeric interlayer. Ambient (white noise and random excitations) and forced vibration (mass shaker) tests were carried out to identify modal parameters.

The paper mainly aims at: i) assessing potential differences in the overall dynamic behavior of the two mockups, likely due to the introduction of acoustic insulation, ii) detecting possible drawbacks of insulation layers on mechanical performances, iii) increasing the knowledge about dynamics of CLT structures.

The results of Operational Modal Analysis (OMA) are presented and the variations in the dynamics between the mockups are discussed. The construction of finite element (FE) models and their calibration – with joint properties variations – are then presented. The outcomes revealed a drop of modal frequencies values (at least 20 %) upon the introduction of elastomeric insulation, whilst no significant alteration was observed in the mode shapes. Model updating based on the FE models demonstrated that the dynamic response and the frequency variations were mostly associated with wall-to-wall and wall-to-diaphragms joints, and hold-down connections.

1. Introduction

The use of timber components, especially Cross-Laminated Timber (CLT), in the construction market has significantly increased in recent years [1]. However, the novelty of the system also implies some uncertainties in the construction design, which are linked to the limited experiences collected so far. For instance, few studies have been addressed to the characterization of its dynamic behavior. Although dry assembling technique of timber structures could produce a strongly nonlinear behavior under seismic shocks, modal analysis could help the understanding of the dynamic response in terms of natural frequencies, damping ratio and mode shapes. Some studies which included both dynamic characterization and model updating have been published by Aloisio et al., 2020, Mugabo et al.,

* Corresponding author.
E-mail addresses: matteo.salvalaggio@unipd.it (M. Salvalaggio), filippo.lorenzoni@unipd.it (F. Lorenzoni), mariarosa.valluzzi@unipd.it (M.R. Valluzzi).
[1] Present address: Institute for Sustainability and Innovation in Structures Engineering (ISISE), ARISE, Department of Civil Engineering, University of Minho, Guimarães, Portugal; e-mail: matteo.salvalaggio@civil.uminho.pt

https://doi.org/10.1016/j.jobe.2024.109525
Received 13 January 2024; Received in revised form 22 April 2024; Accepted 3 May 2024
Available online 5 May 2024

2019 [2,3], while Reynolds et al., 2015, 2016 [4,5] focused strictly on Ambient Vibration Tests (AVTs). Moreover, while such studies have investigated CLT buildings with finishings or in various stages of construction, they have only partly explored the dynamics of structures entirely made of CLT components (detailed descriptions are reported in Sub-Section 1.1). Hence, there is a need to extend the research in such direction.

Acoustic insulation of dry-assembled CLT structures is often achieved by insertion of elastomeric interlayers (henceforth layers) within panels joints (e.g., wall-to-wall, wall-to-diaphragm) [6]. Their interaction with mechanical behavior has been only partially characterized by Azinović et al., 2021, Kržan and Azinović 2021 [7,8]. Such investigations are described in Sub-Section 1.2.

In such a framework, the aims of the paper concern: i) the dynamic characterization of timber structures without and with acoustic insulation details, i.e., elastomeric layers within joints, ii) the detection of any structural drawbacks due to the use of such acoustic details, iii) the investigation of the dynamics of timber structures without any supplementary finishing, structural components, or supplementary load other than bearing panels. To these ends, an experimental campaign addressed to the dynamic characterization of twin two-story mockups - one with conventional joints (Mockup A) and the other with insulated joints (Mockup B) – was carried out.

The experimental testing was performed through dynamic identification (ID) tests. Excitation of the structure was gradually increased with ambient vibrations, random excitations in space and time, and mass shaker harmonic inputs, without introducing any nonlinear deformations. Operational Modal Analysis (OMA) was applied to extract the modal parameters, i.e., mode shapes, frequencies, and damping ratios. Three OMA techniques were used, i.e., Enhanced Frequency Domain Decomposition (EFDD [9]), Stochastic Subspace Identification (SSI [10]), and poly-reference Least Squares Complex Frequency (pLSCF [11]).

Following, FE models of the twins were constructed in DIANA FEA environment [12]. Parametric sensitivity analyses were carried out to detect target parameters to be adjusted for the calibration of the models, based on the outcomes OMA. In such a way, the impact of incorporating insulation layers within joints on the overall dynamic behavior was estimated. Fig. 1 reports the flow chart of the study presented in this paper.

1.1. *Dynamic behavior of timber structures*

Understanding the dynamic behavior of CLT structures plays a key role in their seismic design, typically relying on response spectrum analysis for new constructions. In this framework, the correct prediction of mode frequencies and associated shapes is fundamental to obtain a good approximation of expected seismic forces and a robust design of structural components.

A simplified analytical formulation for the calculation of first mode frequency, $f_1 = C_1 \cdot H^{0.75}$, where C_1 is a ratio function of structural typology and material, and H is the height of the building, is given in Eurocode 8 [13]. However, detailed component

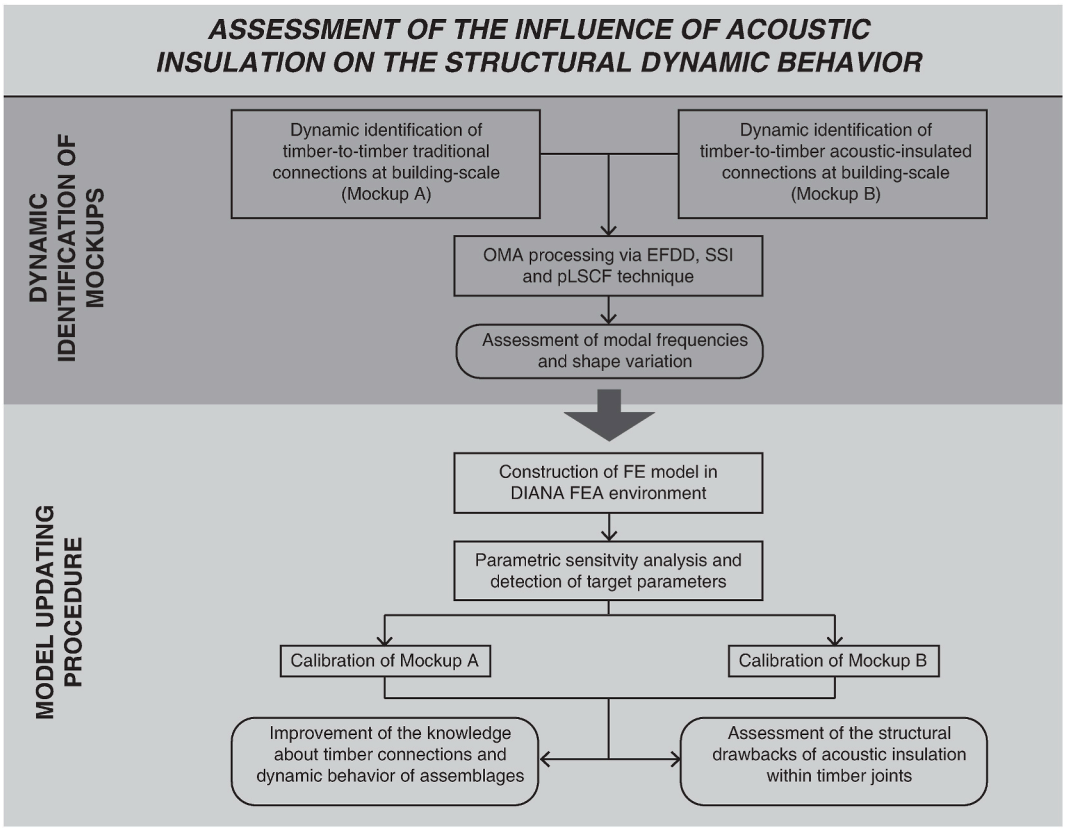

Fig. 1. Flow chart of strategy discussed in the paper.

modeling allows to comprehensively derive the dynamic behavior of CLT structures [14], even when involving unconventional typologies or details (e.g., sound insulated joints). Hence, the collection of experimental data is crucial.

Mugabo et al., 2019 [2] discuss AVTs [15] carried out on a four-story building (i.e., Albina Yard building in Portland, Oregon, USA), made of a mix of Douglas-fir CLT floors, Douglas-fir Glued Laminated Timber (GLT) framing gravity systems (columns and beams), and plywood shear walls with steel hold-downs for the lateral resisting system. The building was complete of structural and non-structural parts, thus all additional masses and stiffnesses beyond wooden ones were taken into account. Ambient environment excitations were used (e.g., road traffic, wind). Two OMA techniques, EFDD and SSI, were used to process the data and estimate the modal parameters. OMA led to the identification of a transverse mode at 2.85 Hz, a longitudinal bending mode at 4.17 Hz, and a torsional mode at 4.24 Hz. Results pointed out, as expected, significant uncertainties in modal damping estimation, as also discussed in Refs. [16–18].

The dynamic identification of the NMBU campus of Norwegian University of Life Science, in Ås, Norway was performed and discussed by Aloisio et al., 2020 [3]. The case study was a 26.9 m-height eight-story CLT building with a rectangular plan (23.21 m × 15.11 m) and an inner core. Walls were monolithic (without any in-plane joints), with high length-to-height ratio. The testing setup consisted of 10 piezoelectric accelerometers. The first two modes identified were translational along transverse and longitudinal directions, at 1.913 and 2.414 Hz, respectively. The third torsional mode was detected at 2.688 Hz. Damping ratios varied from 1.2 % to 1.9 %, with the maximum value related to the first mode. Frequency values were found higher than expected, as if the stiffness was due only to in-plane shear deformability of CLT panels, whilst connections were not stressed enough to activate and deform. Moreover, the authors found that first mode prediction, according to Italian code NTC 2018 [19], aligned well with a C_1 constant equal to 0.0488, close to the one prescribed for masonry structures (i.e., 0.05).

The dynamic behavior of one timber frame and one CLT twin multi-story buildings - identical floor plans, layout and finishings beyond different load-bearing structural system - was studied by Reynolds et al., 2016 [20], in order to assess the structure dynamics differences between the two construction techniques. The similarity of the dynamic responses of the two buildings was high, although the different transfer load concepts (i.e., frame versus walls). However, it should be noted that a reinforced concrete core was part of the buildings, giving a substantial contribution to the overall dynamic response.

In such a framework, the paper introduces a study addressed to the dynamic characterization of isolated CLT structures, without any external influence stemming from additional components or finishes.

1.2. Acoustic insulation layers for timber structures

Shortcomings of timber buildings in satisfying current comfort requirements for acoustic performance manifest in the areas of low-frequency airborne sound insulation and the limitation of structure-borne noise [21,22]. These deficiencies stem from the use of steel connectors in CLT assemblies, which, like many dry-mounted systems, hinder the implementation of soundproofing systems based on component decoupling [23].

The flanking transmission, i.e., the vibration reduction index K_{ij} [24], upon the introduction of sound insulation interlayer was investigated in the case of an isolated X-type CLT connection [25] and a mockup with L- and X-joints [26]. It was found that the decrease of flanking transmission was effective when vibration originated from a lower story to an upper one, whereas it was negligible when the vibration source was within the same slab. Similar studies can be found in Refs. [27–29].

Since panels joints rule the stiffness of CLT assemblages [30], the insertion of elastomeric layers among nails or screws can affect the stiffness and strength of the joints, thus affecting the design of CLT assemblages. A study carried out by Kržan and Azinović, 2021 [7] evaluated the shear and tension/compression (normal) capacity of an angle bracket designed to accommodate a layer for acoustic insulation. The authors discovered that the presence of such a layer embedded in brackets had no significant impact on the bearing and displacement capacity for shear and compression/tensile behaviors. However, it was observed that elastomeric layer bedding affected the stiffness of the connection systems and led to an average reduction of 22 % in shear and 45 % in tension. Furthermore, additional rocking phenomena induced by insulation were recorded. Insulation layers also affected energy dissipation, but the difference between insulated and uninsulated specimens decreased as cycles increased.

An extension of the study [7] was performed by Azinović et al., 2021 [8], where a full-scale CLT wall was examined. It consisted of a 3-layer 249 × 249 × 10 cm CLT panel connected to a 5-layer 14 cm-thick CLT slab, fixed to the base using the two steel angle brackets described in Kržan and Azinović, 2021 [7]. The brackets were fastened with eight full-threaded (FT) 8 × 80 mm screws, while the slab was connected with ten FT 8 × 160 mm screws. The goal of the study was to investigate the cyclic behavior of insulated angle brackets in CLT constructions. Two different groups (four types) of 12.5 mm-thick insulation layer materials were tested as bedding under the wall, ranging from moderately flexible to stiffer options. The insulation for the angle brackets remained constant and was made of 12.5 mm-thick moderately flexible closed-cell polyurethane. The findings indicated that the load-bearing capacity of the wall under vertical stresses remained almost unchanged, but the lateral stiffness was significantly reduced due to insulation layer deformation. Upon the introduction of moderately flexible insulation, the reduction in stiffness reached the 40 %.

Given the limited exploration of the impact of insulated joints on the overall structural behavior, primarily due to previous investigations focusing on component-scale specimens, the paper delves into the dynamic characterization of a CLT mockup specifically equipped with such details.

2. Materials and methods

Two twin building-scale CLT specimens, named Mockup A and Mockup B, were built and equipped with conventional joints (A) and insulated ones, i.e., with elastomeric layers (B).

Mockups were designed to bear gravity and seismic loads expected for the site (i.e., a warehouse of Bozza Legnami s.r.l. in

Villamarzana, Rovigo, in the Italian Veneto region) according to Eurocode 5 [31] and Eurocode 8 [13].

2.1. Description of the mockups

The mockups consisted of twin two-story parallelepiped structures 9.7 m × 4.00 m × 6.14 m (length × width × height). Fig. 2 shows the type plan and section.

The two specimens (Fig. 3a) were characterized as follows.

- Mockup A: conventional wall-to-wall and wall-to-floor joints (i.e., T-joints, L-joints, in-plane joints) with screwed steel brackets (i.e., hold-down and angle brackets);
- Mockup B: insulated wall-to-wall (L- and T-) and wall-to-floor (L- and T-) joints, insulation bedding for panel-to-foundation, panel-to-diaphragm interfaces, and hold-downs (Fig. 3b,c); conventional angle brackets and wall-to-wall in-plane joints.

Fig. 4 resumes and compares the timber-to-timber joints details implemented in the A and B mockups. Layout of Fig. 4a was adopted for T-joints, whereas layout of Fig. 4b was used for L-joints. Layout of Fig. 4c was used for the in-plane wall joints in both mockups. Roof joints consisted of Ø8 × 200 mm PT STS, with an alternate 45° inclination and a spacing of 200 mm; inter-story diaphragm was not provided with any screwed joints. Floor and roof CLT boards were connected to walls by Ø8 × 280 mm PT STS inserted orthogonally (90°) (Fig. 4d) with a spacing of 400 mm. Lintels gravity loads were supported on adjacent walls via a 15 cm-wide mill, while shear forces were resisted by one Ø8 × 280 mm PT STS on each side, inserted at a 45° inclination as illustrated in Fig. 4e.

CLT elements made of C24 raw laminations (a maximum proportion of 10 % C16 is permissible) were used [32]. Table 1 reports their characteristics, according to the producer (i.e., Stora Enso) and codes [31,33]. Vertical walls and roof were made of 10 cm-thick 3-layer CLT panels (Stora Enso C3s 30-40-30 mm), while first diaphragm was made of 14 cm-thick 5-layer ones (Stora Enso C5s 40-20-20-20-40 mm). The average width of panels was equal to 122 cm, with some smaller when needed, as described in Fig. 2. In-plane spline joints (Fig. 2c) were made through 15 cm-wide, 2.7 cm-thick Laminated Veneer Lumber (LVL) [34] joists (i.e., Kerto Q, Table 1) connected with screws to the load bearing CLT panels beneath with a 150 mm spacing. Fastenings were based on flat-head PT steel self-tapping screws (STS), applied without pre-drilling. Table 2 reports their main characteristics. The acoustic insulation consisted of 6 mm-thick anti-vibration stripes made of fibers and granules of recycled styrene-butadiene rubber with non-woven fabric support, hot pressed with polyurethane resin (commercial name Sylpro 6 AD). Table 3 reports the main mechanical and acoustic properties of elastomeric insulation, while Fig. 5 describes its compression law until 10 % strain [35]. An adhesive was used to enhance

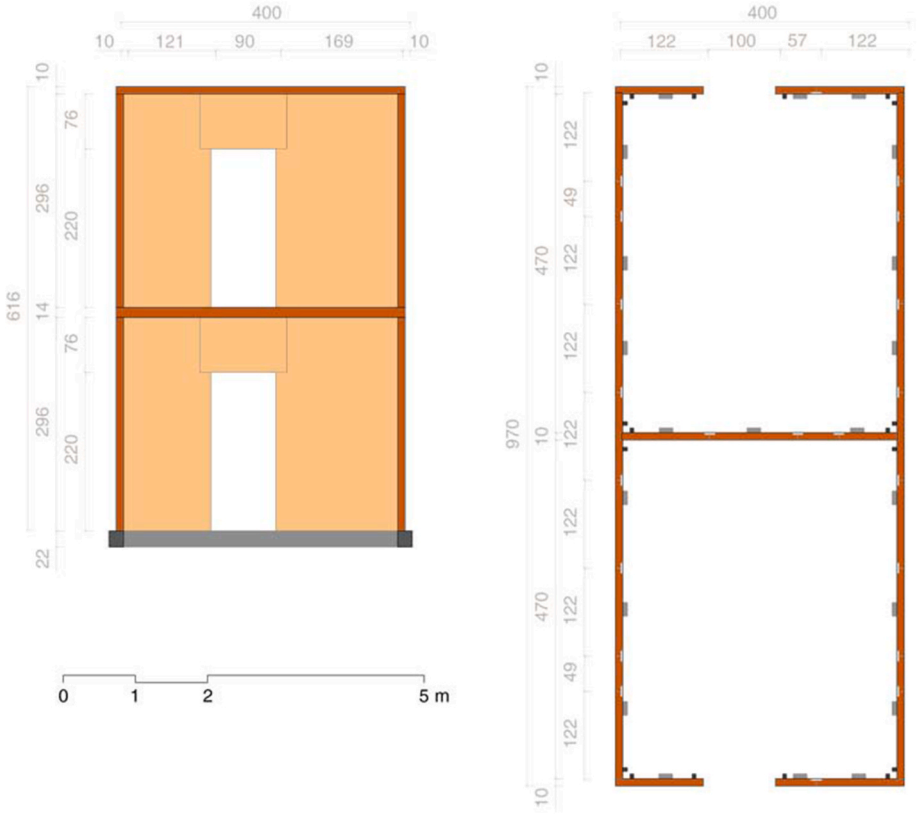

Fig. 2. Type plan and section of mockups (hold-downs in solid black, angle brackets in solid grey).

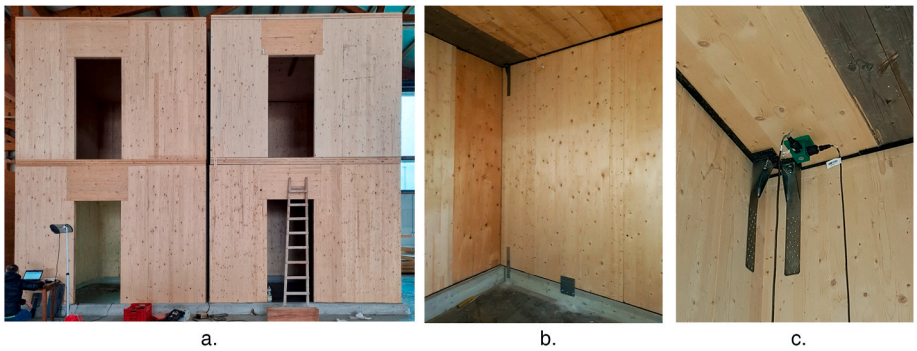

Fig. 3. Views of mockups: a) main façades of mockup A (on the left) and mockup B (on the right); b) details of mockup B wall-to-foundation and wall-to-diaphragm insulation bedding; c) detail of wall-to-diaphragm and hold-down insulation, also with two accelerometers placed.

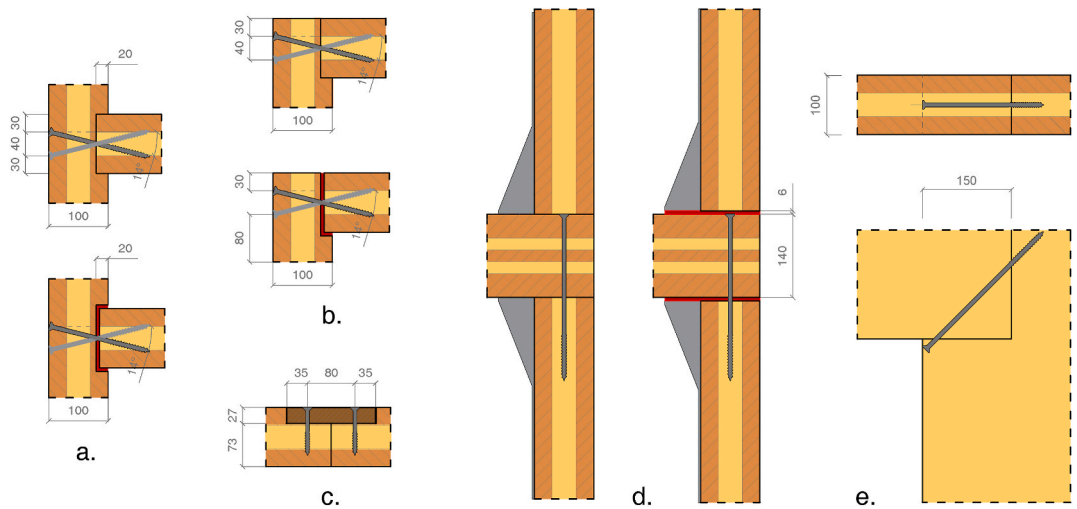

Fig. 4. Timber-to-timber joints layouts, without and with insulation layers (in red): a) wall T-joints; b) wall L-joints; c) wall in-plane spline joints; d) wall-to-diaphragm joint (with hold-down brackets); e) lintel-to-wall joint. (For interpretation of the references to color in this figure legend, the reader is referred to the Web version of this article.)

Table 1
Characteristics of Stora Enso C24 timber boards [32,33] and Kerto Q LVL [34].

Material	Parameter	Value
C24 Timber	Density ρ [kg/m^3]	371
	Grade	C24
	Mean Young's modulus parallel bending $E_{0,mean}$ [MPa]	12500
	Mean Young's modulus perpendicular $E_{90,mean}$ [MPa]	370
	Mean shear modulus perpendicular $G_{090,mean}$ [MPa]	690
	Mean shear modulus parallel $G_{9090,mean}$ [MPa]	50
	Tensile strength perpendicular $f_{t,90,k}$ [MPa]	0.12
	Compressive strength perpendicular $f_{c,90,k}$ [MPa]	2.5
	Shear strength parallel $f_{v,090,k}$ [MPa]	4.0
	Shear strength perpendicular $f_{v,9090,k}$ [MPa]	1.05
Kerto Q LVL	Characteristic density ρ_k [kg/m^3]	480
	Average density ρ_m [kg/m^3]	510
	Shear strength $f_{v,k}$ [MPa]	4.5
	Mean shear modulus G_{mean} [MPa]	600

the bond with CLT components.

The structural masses consisted of CLT panels, steel brackets and connectors. No additional vertical loads, such as floor operating loads, were introduced. Hence, higher mode frequencies compared to operational structures are expected.

Table 2
Characteristics of STS fasteners [36].

Parameter	Steel fasteners		
	PT STS screw type		
	Ø5×80mm	Ø8×200mm	Ø8×240mm
Joint layout	Wall in-plane	Wall T and L	Diaphragm-to-wall
Thread diameter [mm]	5	8	8
Root diameter [mm]	3.40	5.40	5.40
Shank diameter [mm]	3.65	5.80	5.80
Head diameter [mm]	10.00	14.50	14.50
Total length [mm]	80	200	240
Thread length [mm]	40	80	80
Yielding moment My,k [Nmm]	5417	20057	20057
Head penetration stength $f_{head,k}$ [N/mm^2]	10.5	10.5	10.5
Tensile strength $f_{tens,k}$ [kN]	7.9	20.1	20.1

Table 3
Characteristics of Sylpro 6 AD insulation elastomer [35].

Sylpro 6 AD Insulation	
Parameter	Value
Mechanical parameters	
Thickness t [mm]	6
Density ρ [kg/m^3]	800
Compression load at 10 % displacement [kPa]	>90
Acoustic parameters	
Dry dynamic stiffness [MN/m^2]	77
Foot traffic noise reduction ΔL_w [dB]	20

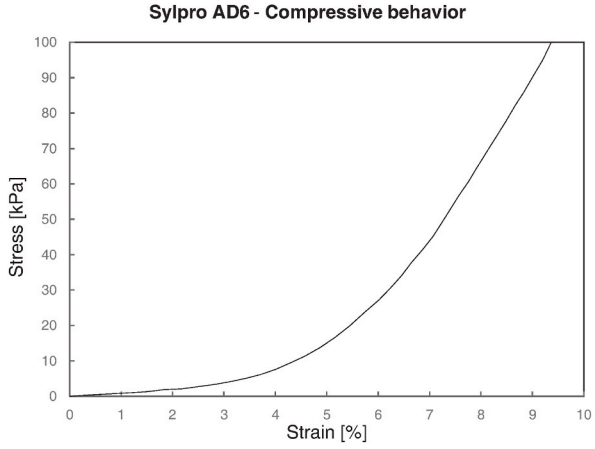

Fig. 5. Compression law of Sylpro 6 AD insulation elastomer until 10 % deformation [35].

Table 4
Steel brackets layout.

Bracket	Number of elements	Position	Number and type of fasteners (per each element)	Anchor bolts	Anchoring binder
Hold-down	16×2 (Inter-story) + 12 (Roof)	Inter-story, Roof	30× FT Screws Ø5×60 mm	M16 5.8	-
Shear bracket plate	21	Foundation	30× FT Screws Ø5×60 mm	2× M12 5.8	Epoxy resin ETA-11/0182
Hold-down plate	16	Foundation	18× FT Screws Ø5×60 mm	M16 5.8 (160 mm depth, c=130)	Epoxy resin ETA-11/0182
Angle bracket	21	Inter-story	36 + 36× FT Screws Ø5×60 mm	–	-

Table 4 describes the steel hold-downs and angle brackets designed according to Eurocodes 8 and 5 [13,31].

2.2. Dynamic identification test setup

ID system consisted of piezoelectric monoaxial accelerometers with a sensitivity of (±10 %)10000 mV/g g and a broadband resolution of 0.00008 g rms, an acquisition unit and coaxial wires. Fig. 6 shows the test setup with the installation of 12 accelerometers, mounted on cubes fastened by screws to the intrados of diaphragms to ensure a rigid connection between sensors and structure. Various input sources were tested, to better excite all modes in the frequency band of interest and thus enhance the detection of structural mode shapes. Beyond ambient vibrations, random excitations were applied through manual pushes of two operators at first floor, to excite the three expected modes, i.e., transversal and longitudinal bending, and torsional. Moreover, a mass shaker harmonic source was positioned above the middle point of the roof and used to furtherly excite the structure with a likely most consistent input [37,38]. Its mass was equal to 2.31 kg with an eccentricity of 14.25 cm.

Records were acquired with a sampling frequency of 200 Hz and a duration of 656 s. Acceleration time series were processed by OMA techniques (EFDD, SSI, and pLSCF) for the extraction of modal parameters. Signals were pre-processed by the application of a Butterworth 3 Hz high-pass filter and a specific algorithm for offset removal. The software SVS Artemis [39] and the Matlab toolbox MACEC [40] were used for modal analysis.

Identification results were validated by comparing the frequency error (D_f) and the mode shapes correlation through the calculation of the Modal Assurance Criterion (*MAC*) index [41].

2.3. Numerical simulation of CLT structures

The understanding of the behavior of CLT mockups and, thus, the effect of insulation, required the construction of a structural model able to simulate their dynamic behavior.

The results of the ID tests were used to assess the mechanical characteristic of CLT assemblages by a numerical model in the FE environment DIANA FEA [12]. The mechanical properties were derived by Eurocode 5 [31] and ETAs [42,43]. The selection, calculation and implementation of such values are reported in Section 3.

The wall loads were simulated using shell distributed density, whereas diaphragms ones were implemented as linear masses along wall-to-diaphragm joints, accounting for plate load distribution. Operational loads were not included, as indicated by the IDs. Eigenvalue analysis implemented in DIANA FEA [12] was performed to detect mode frequencies and associated shapes.

2.3.1. Construction of the FE model

The FE structural model was built - based on the geometry of the mockups - for the simulation of the dynamic behavior (Fig. 7). Discretization was performed according to Christovasilis et al., 2020 [14], by implementing a detailed components modeling [44] with average 15 cm-size orthotropic shell elements for the simulation of CLT panels (11282 4-noded linear Q20SF and 36 3-noded linear T15SF elements), linear interfaces for timber joints with steel fasteners (i.e., wall-to-wall L-, T- and in-plane joints, diaphragm-to-diaphragm in-plane joints, wall-to-lintel, wall-to-diaphragms X- and T-joints for a total of 1934 L16IF linear interface elements); nodal linear springs for foundation hold-downs and angle brackets (39 N6SPR spring elements); 2-noded linear springs for diaphragm and roof ones (65 N12SPR elements). Lintel-to-wall joints were simulated through interface elements, without explicitly modeling the milled junction on wall side.

The deformability of walls bedding was implicitly attributed to brackets, primarily on hold-downs - since the most stressed by vertical loads - and secondarily on angle brackets.

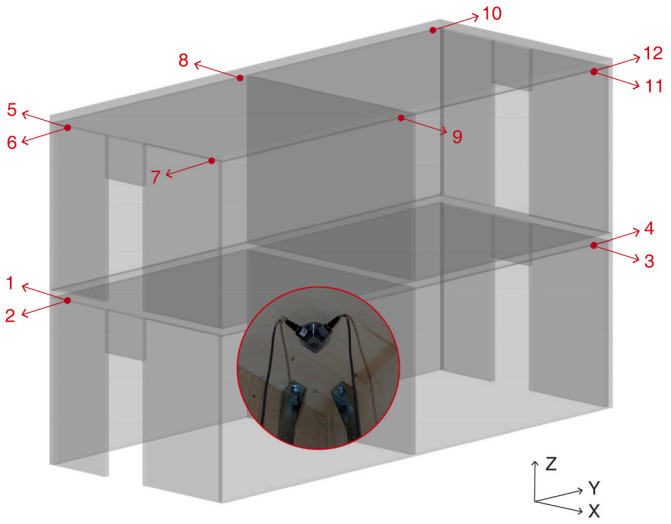

Fig. 6. ID test setup. Detail of accelerometers positioning in the circle.

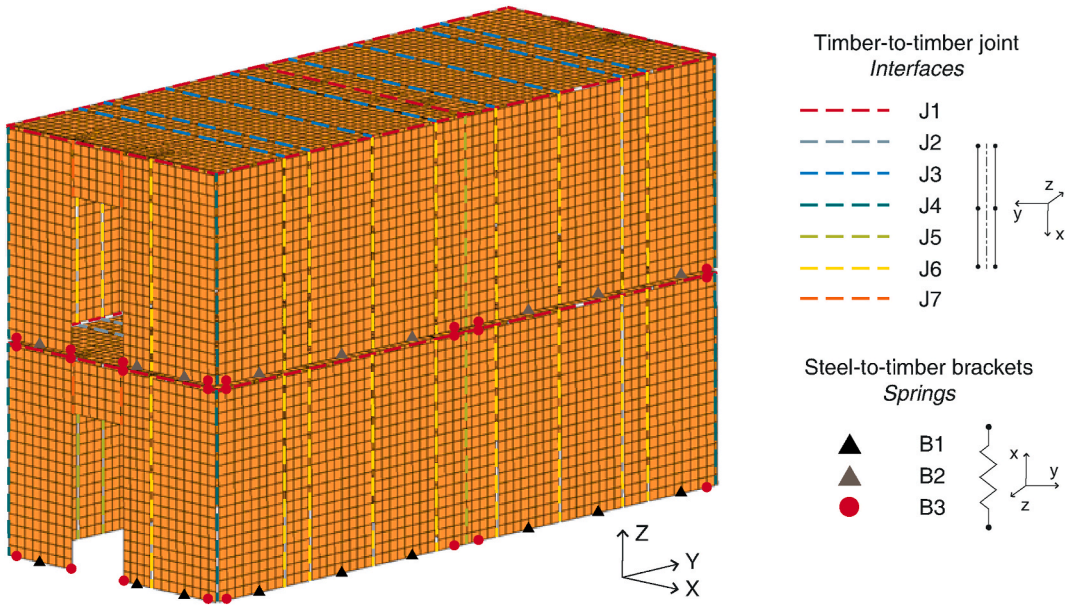

Fig. 7. FE model of the mockups with properties and local axes of spring and interface elements.

2.4. Updating of the FE model

A calibration procedure was implemented to match numerical outputs and experimental results through the adjustment of numerical inputs. Model updating techniques have been widely applied, with automatic, semi-automatic or manual techniques [45–48]. According to Refs. [49,50], the unknows related to the structural characterization could be subdivided into two categories, aleatory and epistemic. In this study, with detailed component-level modeling followed [44,51], sensitivity analyses - aimed at assessing the influence of each unknown - were focused on joints and brackets stiffnesses, treated as aleatory parameters. Density ρ, Young's modulus E and shear modulus G of CLT panels were kept constant, since the material is precast, hence its variability is expected to be low compared to joints one [52,53].

The outcomes of sensitivity analyses allowed the detection of the target parameters to be updated in order to match experimental outcomes. According to Refs. [47,54,55], sensitivity coefficient of parameters can be described as per Equation (1):

$$S_{i,j} = \frac{X_j}{R_i^{FEM}} \cdot \frac{\Delta R_i^{FEM}}{\Delta X_j} \tag{1}$$

where i is the frequency index, j is the parameter index, X_j represents the j-th model parameter and R_i^{FEM} is the i-th analysis output (i.e., mode frequency), and the Δ-the relative variations.

According to Cattari et al., 2021 [49], sensitivity factor S_n, within parameters ranging between a maximum and a minimum values, can be described as per Equation (2):

$$S_n = \frac{R_{max} - R_{min}}{0.5(R_{max} + R_{\min})} \cdot \frac{0.5(P_{max} + P_{\min})}{P_{max} - P_{min}} \tag{2}$$

where $R_{\max}$ and $R_{\min}$ are the maximum and minimum response of the model in terms of frequency; $P_{\max}$ and $P_{\min}$ are the maximum and minimum values adopted for the parameter.

According to Equations (1) and (2), sensitivity coefficient and factors were calculated for the 1.2 multiplier and the 0.3–2 multiplier range, respectively. Based on parametric analysis outcomes, results were compared to experimental OMA outputs by calculating MAC indexes and frequency discrepancies.

Some of the values-set generated by sensitivity analyses were chosen as pre-calibrated models to be furtherly manually updated, in order to achieve the model calibration. Based on multipliers between 0.3 and 2, the objective function was constructed as per Equation (3):

$$f(x) = \sum_{i=1}^{M} \left[\alpha_i \left(\frac{f^{EXP} - f^{DR}}{f^{EXP}} \right)^2 + \beta_i \left(\frac{1 - \sqrt{MAC_i}}{MAC_i} \right) \right] \tag{3}$$

where $M = 3$, $\alpha_i = 1$ and $\beta_i = 0.5$ [47]. Sets which provided the minimum values were selected as the calibrated ones.

3. Estimation of mechanical properties

The numerical implementation of timber panels is crucial for the global simulation of wooden building. Timber panels behavior - and particularly CLT ones - can be described through component or phenomenological methods [1,44,56]. In this paper the second approach is used, therefore the discussion here reported is limited to that.

References about the calculation of CLT panel properties starting from wooden layer ones can be found in Refs. [57–59]. The calculation of the stiffness values was done according to the so-called Homogenised Orthotropic plane stress Blass reduced cross Section (HOBS) method [58–60], based on the composite theory and k_i composition factors in function of the orthotropic description of bidimensional elements (E_x, E_y, E_z, G_{xy}, G_{xz}, G_{yz}). However, since the influence of out-of-plane shear moduli G_{xz} and G_{yz} are secondary with respect to the in-plane one G_{xy}, the same value was given to the three ($G_{xy} = G_{xz} = G_{yz}$) [14,59]. Table 5 reports the properties of CLT panels derived accordingly.

The stiffness estimation of fastened (dowel-type) timber-to-timber and steel-to-timber joints are based on the so-called slip modulus K_{ser}, according to Refs. [31,61]. In the case of steel-to- and concrete-to- timber joints, K_{ser} could be estimated [31] as up to:

$$K_{ser,steel-to-timber} \approx 2 \cdot K_{ser,timber-to-timber} \tag{4}$$

Although shear-load fastened connections (e.g., screws and nails) have been widely investigated (e.g., Crocetti et al. 2016 [62]) and analytical estimation methods collected within national and international codes [31,61], the characterization of axially-loaded fastened joint stiffness has been only partially explored.

Equations provided by ETA-11/0030 [42] are able to estimate with a good approximation the experimental performances of axially loaded 45° and 30° inclined screws [52]. Moreover, the axial stiffness was found usually higher than shear-slip one. Hence, Equations (5) and (6) according to fasteners producer ETA [42] were used in this study.

$$K_{ser,ax\ (softwood)} = 25 \cdot d \cdot l_{ef} \tag{5}$$

$$K_{ser,ax\ (hardwood)} = 30 \cdot d \cdot l_{ef} \tag{6}$$

Experimental evidences have clarified that hold-downs' shear strength is low compared to the tensile one (about one-tenth), while angle brackets' tensile strength is comparable to shear one [63,64]. However, the tensile and shear stiffnesses are comparable each other in both cases. Therefore, the calculation of the panel uplift resistance must consider the angle brackets contribution.

In this study, K_{ser} values according to Eurocode 5 [31] were preliminary adopted.

The stiffness of steel-to-timber brackets, modeled as linear springs in N/mm, was derived by summing the K_{ser} contribution of each screw according to Eurocode 5 [31], as per Equation (7), since its effectiveness in the prediction of experimental values was noticed in Refs. [65,66]:

$$K_{ser} = \rho^{1.5} \cdot d/23 \tag{7}$$

Hold down shear stiffness was set equal to 2/3 of axial one, whereas shear brackets tensile and shear stiffnesses were assumed equal, as observed in the specimens tested in Refs. [63,64]. Base and inter-story hold-down brackets were given the same property values.

The shear $j_{k,shear}$ and axial $j_{k,ax}$ interface stiffnesses of timber-to-timber joints, modeled as linear interfaces between shell elements, and expressed in N/mm^3, were calculated as per Equations (8) and (9):

$$j_{k,shear} = \frac{n \cdot K_{ser}}{t \cdot h} = \frac{n \cdot K_{ser}}{A_c} \tag{8}$$

$$j_{k,ax} = \frac{n \cdot K_{ser,ax}}{t \cdot h} = \frac{n \cdot K_{ser,ax}}{A_c} \tag{9}$$

where n is the number of connectors, t the thickness of the panel and h its height, and A_c the contact area between the two joints.

The axial stiffness $K_{ser,ax}$ was derived as per Equations (5) and (6). An arbitrary value of 1 N/mm^3 was used to prevent local out-of-plane phenomena from arising in L-, T- and in-plane wall joints, floor and roof joints, since they could alter mode shapes. This assumption was in line with overall box behavior shown by the specimen in IDs.

In the case of in-plane wall joints, where screws intersect both CLT and LVL elements, an equivalent density was considered for K_{ser} values, as per Eq. 7.1 of [31] reported in Eq. (10):

$$\rho_m = \sqrt{\rho_{m,1}\rho_{m,2}} \tag{10}$$

Table 5
Linear properties of CLT panels used in the Mockups (x is the in-plane direction parallel to grain of outer layers, y the orthogonal one, z the out-of-plane direction, see Fig. 4).

CLT panel layers	Thickness [cm]	E_x [MPa]	E_y [MPa]	E_z [MPa]	G_{xy}, G_{xz}, G_{zy} [MPa]
3	10	7667	5250	417	690
5	14	9047	3869	417	690

Since the floor joints were not provided with any fastened connections and rely only on components friction, a value equal to 0.001 N/mm^3 along shear planes was preliminarily assumed.

Table 9 summarizes the stiffness parameters estimations for conventional joints since the characterization of insulated ones is one of the aims of this paper.

Since the mechanical characterization of sound-insulated joints is still unexplored for the most and analytical predictions have not been provided in codes or technical documents, preliminary evaluations for insulated joints were not considered, and were estimated only upon the model updating procedure. However, based on findings [7,8] discussed in Sub-Section 1.2, the stiffness of sound-insulated joints are expected to be lower compared to conventional ones, and hence dynamic behavior of Mockup B altered, especially for frequency values of mode shapes sensitive to insulated joints properties.

4. Results and discussion

4.1. OMA results

The first three principal modes identified for both mockups from modal analysis are: i) transverse bending (Fig. 8a), ii) torsional (Fig. 8b) and iii) longitudinal bending (Fig. 8c). The natural frequencies detected varied between the two mockups, instead.

The modal frequencies and damping ratios identified through OMA applied to Mockup A and B are resumed in Table 6 and Table 7, respectively. They revealed a good consistence among the various inputs (i.e., AVT, random excitations and mass shaker). Frequency values were slightly lower for pLSCF, whereas a major variability was found in damping ratios, as already observed in Mugabo et al. 2019 [2]. The higher values were usually given by SSI, whereas pLSCF had the lowest ones (as noticed by Brownjohn et al. 2010 [67]). Although the given differences among the three techniques, some observations can be done within each one. Damping ratios due to random excitations were higher than AVT ones. Instead, the ones recorded by mass shaker were remarkably lower.

The comparison of the OMA outcomes of Mockup A and Mockup B led to the assessment of the differences on the dynamic response upon the introduction of insulation layers within joints.

Fig. 9 reports a summary of the natural frequencies extracted. A decrease of such values was recorded between the mockups, with a quite constant gap among the various OMA techniques and input sources, as noticeable in Table 8. In terms of frequency discrepancy, the percentages vary between the 30 % and 20 %, with highest differences in the first mode. Since the masses and the geometries of the two mockups are equivalent, the frequency drop was believed to be associated to structural stiffness.

The differences between mode shapes of Mockup A and B were assessed by means of MAC indexes comparison (Table 8). The consistency among the various inputs was good, especially for the first mode shape. MAC indexes exceeded 0.9 for both AVT and random excitations and surpassed 0.8 for the mass shaker. Damping ratios did not show a consistent variation to be associated with the introduction of insulation.

4.2. Model updating

The outcomes of eigenvalue analysis associated with preliminary analytical properties, in terms of mode shapes, are presented in Fig. 10, whereas the corresponding frequencies were equal to 7.05 Hz, 8.66 Hz, 10.73 Hz. The comparison between the experimental and preliminary numerical outcomes of Mockup A shows the underestimation of frequency values by the numerical model, which were closer to the Mockup B. However, it should be considered that brackets stiffnesses in Table 9 were conservative (as discussed in Section 3), since it is allowed to double the value of timber-to-timber fastened joints in case of steel-to-timber joints according to Eurocode 5 [31] (Equation (4)).

4.2.1. Sensitivity analysis

Sensitivity coefficient (Equation (1)) and factors (Equation (2)) were calculated, for a 1.2 multiplier and a 0.3–2 multiplier range, respectively. Fig. 11 resumes the values found. These suggested that in-plane wall-to-wall joints ruled the frequency variations,

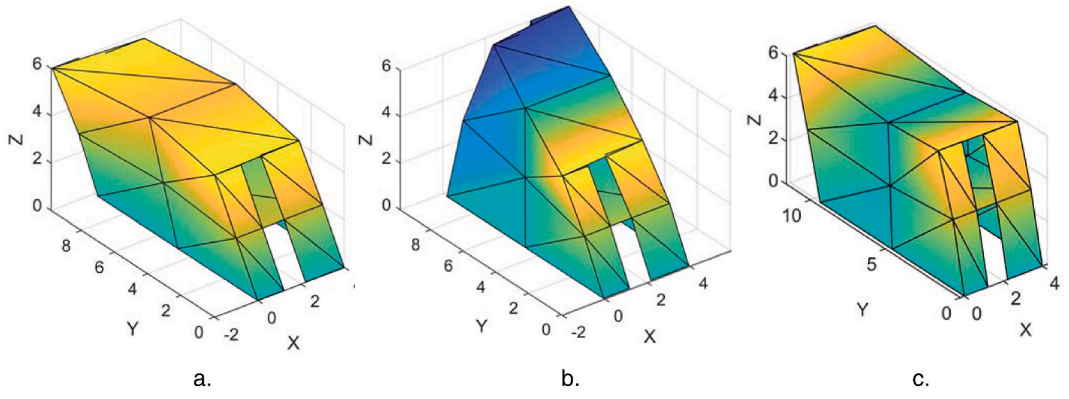

Fig. 8. Mode shapes calculated by the MACEC toolbox [40] for Ambient Vibrations: a) transverse bending, b) torsional, c) longitudinal bending (higher positive normalized value in yellow, lower negative value in blue). (For interpretation of the references to color in this figure legend, the reader is referred to the Web version of this article.)

Table 6
Mode frequencies and damping ratios of Mockup A based on AVT, random excitations and mass shaker, according to EFDD, SSI-UPCX and pLSCF OMA techniques.

Mode	Mockup A								
	Ambient vibrations			Random excitations			Mass shaker		
	EFDD	SSI	pLSCF	EFDD	SSI	pLSCF	FDD	SSI	pLSCF
	Frequency [Hz]								
1	8.71	8.74	8.67	8.62	8.62	8.66	8.34	8.38	8.01
2	10.89	10.92	10.83	10.80	10.76	10.77	–	10.16	10.02
3	16.74	16.95	16.91	16.7	17.38	16.85	–	–	16.15
	Damping ratio ξ [−]								
1	3.42 %	3.41 %	2.26 %	3.76 %	4.08 %	2.86 %	–	0.77 %	0.72 %
2	1.53 %	2.48 %	1.31 %	1.98 %	1.81 %	1.03 %	–	0.42 %	0.53 %
3	2.64 %	3.32 %	1.33 %	3.18 %	5.13 %	3.57 %	–	–	0.11 %

Table 7
Mode frequencies and damping ratios of Mockup B based on AVT, random excitations and mass shaker, according to EFDD, SSI-UPCX and pLSCF OMA techniques.

Mode	Mockup B								
	Ambient vibrations			Random excitations			Mass shaker		
	EFDD	SSI	pLSCF	EFDD	SSI	pLSCF	FDD	SSI	pLSCF
	Frequency [Hz]								
1	6.10	6.08	6.15	6.09	6.1855	6.05	5.66	5.67	5.90
2	7.85	7.78	7.81	7.58	–	7.54	6.8	6.80	–
3	13.50	13.60	13.14	13.60	13.26	13.28	13.1	–	–
	Damping ratio ξ [−]								
1	3.09 %	5.88 %	1.61 %	2.80 %	7.36 %	2.78 %	–	0.18 %	0.20 %
2	1.17 %	2.37 %	0.60 %	2.39 %	–	2.01 %	–	0.78 %	–
3	2.97 %	2.86 %	0.85 %	1.98 %	6.68 %	2.37 %	–	–	–

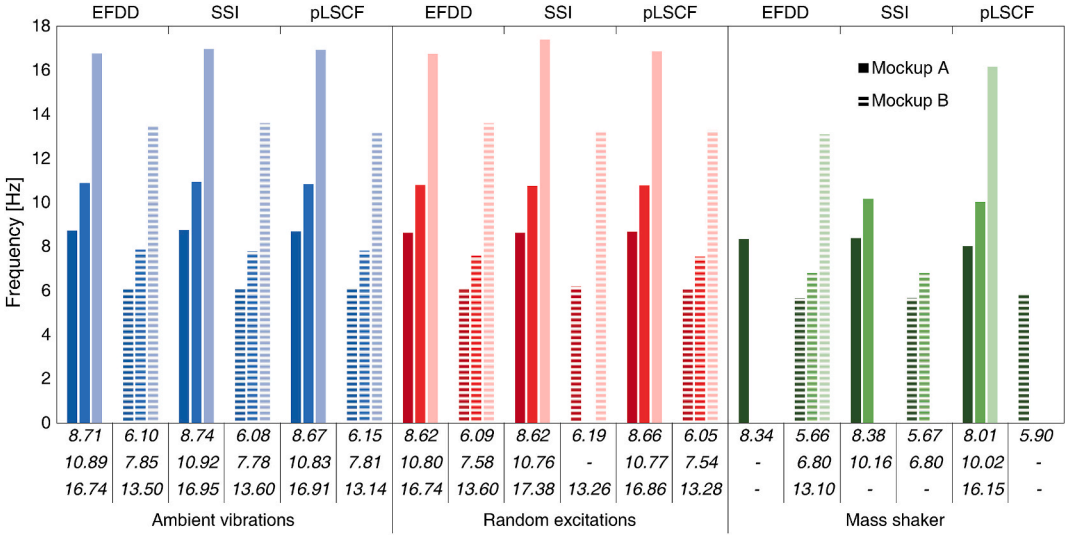

Fig. 9. Mode frequencies [Hz] calculated for Mockup A (full color) and B (hatched color), according to OMA techniques and ambient vibrations (blue), random excitations (red), harmonic mass shaker input (green). (For interpretation of the references to color in this figure legend, the reader is referred to the Web version of this article.)

especially for torsional and longitudinal bending modes. Transverse bending was influenced for the most by the stiffness of the in-plane wall-to-wall joints, and then hold-downs stiffness, floor joints, wall-to-diaphragms joints, floor joints, wall T-joints and foundation shear brackets.

Torsional shape was strongly affected by wall in-plane joints, whilst wall-to-diaphragms and inner-diaphragms joints accounted for about the half. Remaining parameters had negligible influence.

Longitudinal bending frequency was especially affected by wall-to-wall in-plane joints stiffness, whereas other parameters contributions were significantly lower.

Table 8
Frequency discrepancy, MAC indexes between Mockup A and B.

Mode	Ambient vibrations			Random excitations			Mass shaker		
	EFDD	SSI	pLSCF	EFDD	SSI	pLSCF	EFDD	SSI	pLSCF
	Df [%] Mockup A-B								
1	29.94 %	30.47 %	29.04 %	29.37 %	28.23 %	30.10 %	32.13 %	32.30 %	26.34 %
2	27.88 %	28.76 %	27.89 %	29.78 %	–	29.95 %	–	33.07 %	–
3	19.36 %	19.79 %	22.31 %	18.74 %	23.71 %	21.19 %	–	–	–
	MAC [−] Mockup A-B								
1	0.96	0.96	0.93	0.97	0.92	0.96	0.82	0.81	0.81
2	0.92	0.81	0.67	0.92	–	0.93	–	0.74	–
3	0.87	0.85	0.86	0.90	0.87	0.89	–	–	–

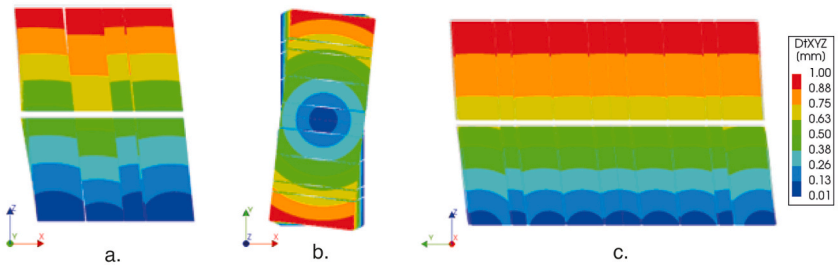

Fig. 10. Typological numerical mode shape (shrink visualization): a) transverse bending; b) torsional; c) longitudinal bending.

Based on Equation (3), per each parameter, points which satisfied minimization of the function were detected and then manually adjusted until the achievement of a satisfying updating.

The mechanical parameters of calibrated models are reported in Table 9. A noticeable discrepancy between Mockup A and B was detected. Values of hold-downs for Mockup A were higher than Mockup B, but still lower than the one of Equation (4). The same values needed to be reduced for Mockup B, where also insulation bedding is included. Lower gaps were found for angle brackets. Since it was reported about 50 % and 40 % reduction of tensile and shear stiffnesses for angle brackets [7], the outcomes of model updating could be considered consistent. However, it was necessary to reduce of a 30 % the in-plane wall joints stiffness to match frequency loss of Mockup B respect to Mockup A. Since CLT panels assembling is a complex procedure with a consistent number of operations and joints, some variability could be found even when same design is followed. Moreover, it must be noticed that the values adopted aimed at calibrating the dynamic outcomes of the structure, and they can significantly differ from the ones obtained through static procedures [68]. Additionally, parameters to which mode shapes were not sensitive could not undergo an updating procedure, meaning their values cannot be validated from a structural point of view.

Table 10 and Fig. 12 summarize the results of calibration. The updating procedure worked well for the first and second modes (i.e., transverse bending and torsional), with numerical frequencies (D_f equals to 2.5 % and 6.85 % for the first and 7.9 % and 0.46 % for the second, for Mockups A and B respectively) and mode shapes close to experimental ones. Although the MAC index was higher than 0.94, the third mode frequency gap remained higher than 20 %. However, since the third experimental frequency was very high, structural interest was believed minor compared to the other two. Moreover, similar discrepancy was found in the calibration of CLT structures dynamic behavior [2].

5. Conclusions

The investigation of two building-scale specimens (about 4 × 9 × 6 m), named Mockup A and B, for conventional and acoustic insulated solutions, respectively, led to the assessment of the effects of such details in the dynamic behavior of a CLT structure. Dynamic identification tests were performed on both mockups, applying various excitation input (i.e., ambient vibrations, random excitations, harmonic mass shaker). According to the main aims of the study discussed in Section 1, the following conclusions can be drawn.

- The adoption of sound-insulation induced a drop between 30 % and 20 % on mode frequencies, especially for the first one, whereas the mode shapes were found unaltered for the most;
- parametric analyses showed that the model was sensitive especially to in-plane wall-to-wall joints, wall-to-diaphragm joints, and hold-down stiffnesses. Thus, the dynamic behavior of specimens is believed to be related to the contributions of inter-story insulation (wall-to-diaphragms T-joints) and hold-down brackets for the most;
- the assessment of the variation between mockups calibrated properties allowed to derive the influence of insulation on the dynamic stiffness properties. Insulated diaphragm-to-wall joints stiffness was found to be 30 % of conventional ones; insulated hold-downs

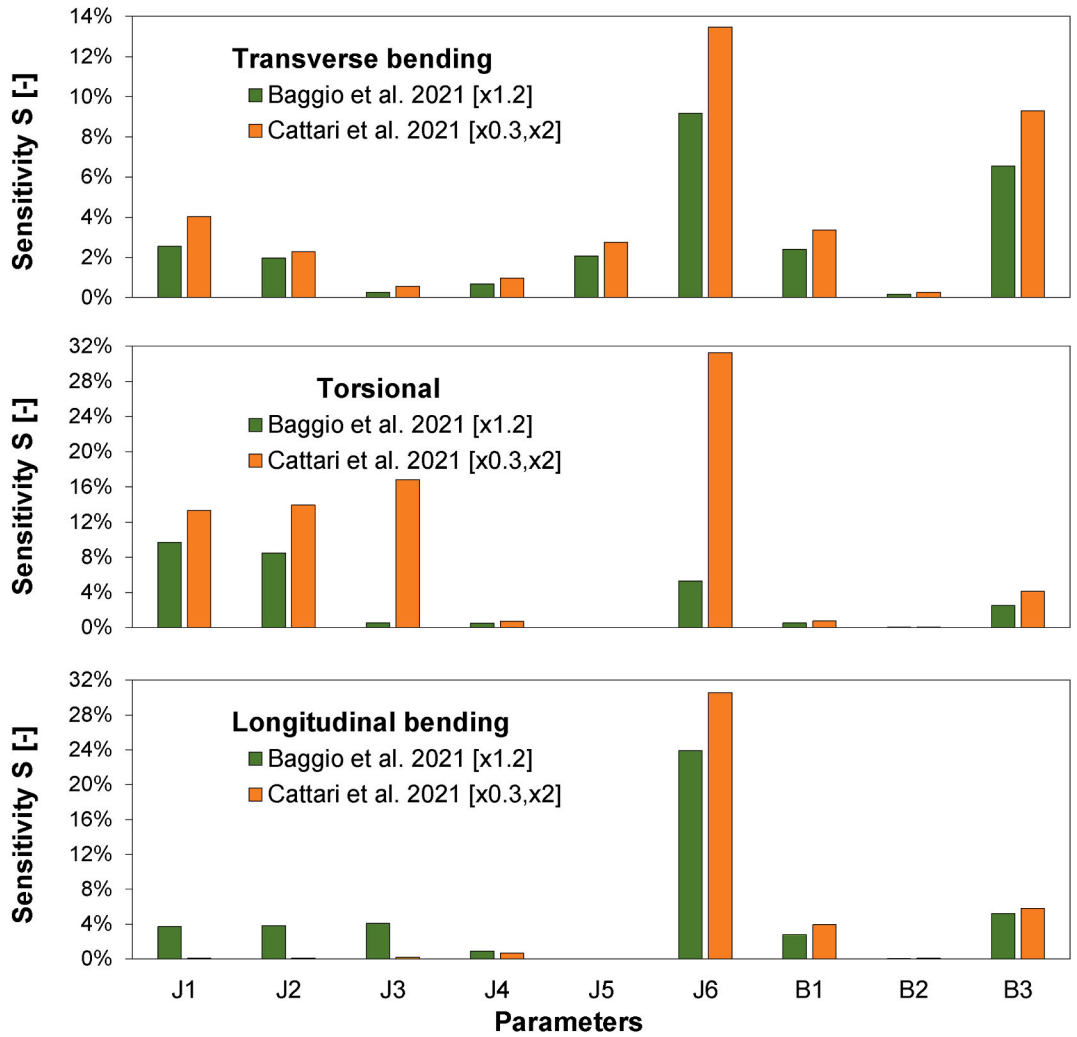

Fig. 11. Sensitivity coefficients and factors of transverse bending, torsional and longitudinal bending modes.

stiffness was about 30 % of conventional ones. These appear in line with [8], where about 60 % stiffness loss for lateral stiffness was detected. Moreover, wall-to-wall in-plane joints had to be driven to a 35 % gap, especially for modes 2 and 3. Thus, it can be concluded that frequency gap between the two samples, A and B, is expected to be related to both insulation and discrepancies in the assembling of the Mockups;

- AVT and random excitations brought to similar outcomes, whereas mass shaker detected slightly lower frequency values, for both mockups;
- the preliminary numerical model with parameters derived by Refs. [31,42] underestimated the experimental frequencies of both mockups.

The study confirms the findings in such field [7,8] and enhances the need to consider the decrease of natural frequencies and alteration of associated response to dynamic loads induced by acoustic insulation. Indeed, the frequencies shift can affect the design seismic forces based on response spectra. The linear stiffness decrease could affect also ductility properties, although load-bearing capacities were found unaltered [7,8]. Hence, the q-factor - estimated close to 3 for conventional assembling techniques [69,70] – could potentially be updated and reduced. To this end, further investigations, e.g., quasi-static and shaking table tests, on full-scale CLT specimens should be performed. Additionally, several other aspects of CLT structures following the introduction of insulation need to be evaluated: i) conducting dynamic characterization in consideration of operational floor masses and potential upper-story loads, ii) examining the impact of different types of insulation interlayers, and iii) investigating specific mechanical details that can mitigate the structural decoupling caused by insulation. Upon achieving a comprehensive characterization of sound-insulated systems, updated recommendations could be provided and further research on enhanced sound-insulation details and systems be developed.

Table 9
Mechanical parameters of Mockup A and B for preliminary and calibrated models. Reference axes for spring and interface elements according to Fig. 7.

Connection category	Stiffness parameter		Preliminary analytical estimation			Final calibrated values					
						Mockup A			Mockup B		
			x	y	z	x	y	z	x	y	z
Timber-to-timber joints (interfaces)	J_1	Wall-to-Floor and Wall-to-Roof [N/mm^3]	0.067	1	0.067	0.1 (+50 %)	1	0.1 (+50 %)	0.033 (-50 %)	1	0.033 (-50 %)
	J_2	Floor joints [N/mm^3]	0.001	1	0.001	0.001	1	0.001	0.001	1	0.001
	J_3	Roof Joints [N/mm^3]	0.067	1	0.96	0.067	1	0.96	0.067	1	0.96
	J_4	L-joints [N/mm^3]	0.249	1	0.249	0.249	1	0.249	0.249	1	0.249
	J_5	T-joints [N/mm^3]	0.249	1	0.249	0.249	1	0.249	0.249	1	0.249
	J_6	Wall in-plane joints [N/mm^3]	0.123	0.755	1	0.17 (+32 %)	0.755	1	0.11 (-15 %)	0.755	1
	J_7	Lintel-to-wall joints [N/mm^3]	0.067	1	0.067	0.067	1	0.067	0.067	1	0.067
Steel-to-timber brackets (springs)	B_1	Plate shear bracket (Foundation) [N/mm]	46604	46604	46604	60000 (+28 %)	60000 (+28 %)	60000 (+28 %)	35000 (-25 %)	35000 (-25 %)	35000 (-25 %)
	B_2	Angle shear bracket [N/mm]	55924	55924	55924	60000 (+10 %)	60000 (+10 %)	60000 (+10 %)	50000 (-10 %)	50000 (-10 %)	50000 (-10 %)
	B_3	Hold down [N/mm]	46604	30000	30000	110000 (+140 %)	50000 (+66 %)	50000 (+66 %)	35000 (-25 %)	22500 (-25 %)	22500 (-25 %)

Table 10
Comparison of experimental and calibrated numerical modal outcomes for Mockup A and B.

Frequency [Hz]				
Preliminary	Experimental		Calibrated numerical	
	Mockup A	Mockup B	Mockup A	Mockup B
7.05	8.71	6.10	8.49	6.52
8.66	10.88	7.85	10.01	7.89
10.73	16.74	13.6	13.3	10.33

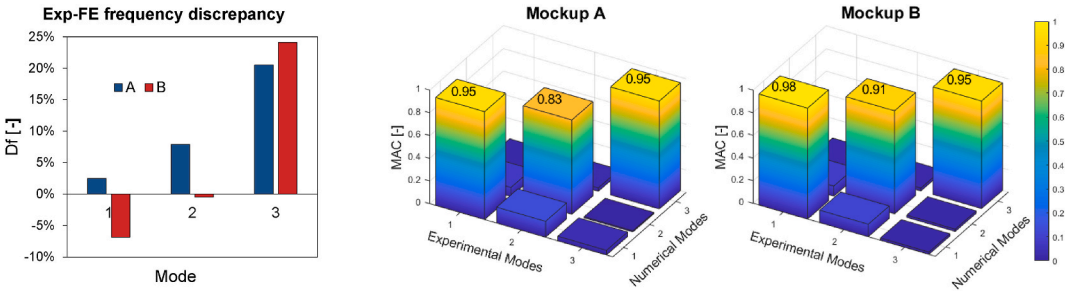

Fig. 12. Experimental-numerical frequency discrepancies and MAC indexes for Mockup A and B.

Funding

This research was mainly funded by the CORE-WOOD (COmpetitive REpositioning of WOOD sector) Italian project, in the framework of POR-FESR 2014–2020 Line 1 Action 1.1.4 of the Veneto Region.

Compliance with ethical standards

The authors declare that they have no conflict of interest.

CRediT authorship contribution statement

Matteo Salvalaggio: Writing – review & editing, Writing – original draft, Visualization, Validation, Methodology, Formal analysis, Data curation, Conceptualization. **Filippo Lorenzoni:** Writing – review & editing, Validation, Supervision, Methodology, Investigation, Formal analysis. **Maria Rosa Valluzzi:** Writing – review & editing, Supervision, Resources, Project administration, Methodology,

Funding acquisition, Conceptualization.

Declaration of competing interest

The authors declare that they have no known competing financial interests or personal relationships that could have appeared to influence the work reported in this paper.

Data availability

Data will be made available on request.

Acknowledgements

The authors wish to thank Mr. E. Bozza and Bozza Legnami s.r.l. for providing the CLT components and assembling the mockups; Eng. A. Caprino, Eng. M. Vettore, Eng. A. Zenari and Eng. F. Zanotto for their contribution in the execution of investigations and processing of data.

References

[1] A. Sandoli, C. D'Ambra, C. Ceraldi, B. Calderoni, A. Prota, Sustainable cross-laminated timber structures in a seismic area: overview and future trends, Appl. Sci. 11 (2021) 2078, https://doi.org/10.3390/app11052078.
[2] I. Mugabo, A.R. Barbosa, M. Riggio, Dynamic characterization and vibration analysis of a four-story mass timber building, Frontiers in Built Environment 5 (2019), https://doi.org/10.3389/fbuil.2019.00086.
[3] A. Aloisio, D. Pasca, R. Tomasi, M. Fragiacomo, Dynamic identification and model updating of an eight-storey CLT building, Eng. Struct. 213 (2020) 110593, https://doi.org/10.1016/j.engstruct.2020.110593.
[4] T. Reynolds, R. Harris, W.S. Chang, J. Bregulla, J. Bawcombe, Ambient vibration tests of a cross-laminated timber building, Proc. Inst. Civ. Eng.: Construction Materials 168 (2015) 121–131, https://doi.org/10.1680/coma.14.00047.
[5] T. Reynolds, D. Casagrande, R. Tomasi, Comparison of multi-storey cross-laminated timber and timber frame buildings by in situ modal analysis, Construct. Build. Mater. 102 (2016) 1009–1017, https://doi.org/10.1016/j.conbuildmat.2015.09.056.
[6] A. Di Bella, M. Mitrovic, Acoustic characteristics of cross-laminated timber systems, Sustainability 12 (2020), https://doi.org/10.3390/su12145612.
[7] M. Kržan, B. Azinović, Cyclic response of insulated steel angle brackets used for cross-laminated timber connections, European Journal of Wood and Wood Products (2021), https://doi.org/10.1007/s00107-020-01643-5.
[8] B. Azinović, T. Pazlar, M. Kržan, The influence of flexible sound insulation layers on the seismic performance of cross laminated timber walls, J. Build. Eng. 43 (2021), https://doi.org/10.1016/j.jobe.2021.103183.
[9] R. Brincker, C. Ventura, P. Andersen, Damping estimation by frequency domain decomposition, in: Proceedings of the IMAC 19, International Modal Analysis Conference, Kissimmee, Florida, USA, 2001.
[10] P. Van Overschee, B. De Moor, Subspace Identification for Linear Systems: Theory - Implementation - Applications, Kluwer Academic Publishers, Dordrecht, Netherlands, 1996.
[11] B. Peeters, H. Van der Auweraer, POLYMAX: a revolution in operational modal analysis, in: Proc. 1st International Operational Modal Analysis Conference (IOMAC), Copenhagen, Denmark, 2005, pp. 45–51.
[12] DIANA FEA 10.5, 2021.
[13] EN 1998:2004 + A1, Eurocode 8: Design of Structures for Earthquake Resistance - Part 1: General Rules, Seismic Actions and Rules for Buildings, 2013.
[14] I.P. Christovasilis, L. Riparbelli, G. Rinaldin, G. Tamagnone, Methods for practice-oriented linear analysis in seismic design of Cross Laminated Timber buildings, Soil Dynam. Earthq. Eng. 128 (2020) 105869, https://doi.org/10.1016/j.soildyn.2019.105869.
[15] I. Mugabo, A.R. Barbosa, M. Riggio, J. Batti, Ambient vibration measurement data of a four-story mass timber building, Frontiers in Built Environment 5 (2019) 1–4, https://doi.org/10.3389/fbuil.2019.00067.
[16] F. Magalhães, Á. Cunha, E. Caetano, R. Brincker, Damping estimation using free decays and ambient vibration tests, Mech. Syst. Signal Process. 24 (2010) 1274–1290, https://doi.org/10.1016/j.ymssp.2009.02.011.
[17] B. Moaveni, A.R. Barbosa, J.P. Conte, F.M. Hemez, Uncertainty analysis of system identification results obtained for a seven-story building slice tested on the UCSD-NEES shake table, Struct. Control Health Monit. 21 (2014) 466–483, https://doi.org/10.1002/stc.1577.
[18] H. Yu, M.A. Mohammed, M.E. Mohammadi, B. Moaveni, A.R. Barbosa, A. Stavridis, R.L. Wood, Structural identification of an 18-story RC building in Nepal using post-earthquake ambient vibration and lidar data, Frontiers in Built Environment 3 (2017), https://doi.org/10.3389/fbuil.2017.00011.
[19] Ministero delle Infrastrutture e dei Trasporti, Decreto Ministeriale 17 Gennaio 2018 - Aggiornamento delle "Norme Tecniche Per le Costruzioni," Italy, 2018.
[20] T. Reynolds, D. Casagrande, R. Tomasi, Comparison of multi-storey cross-laminated timber and timber frame buildings by in situ modal analysis, Construct. Build. Mater. 102 (2016) 1009–1017, https://doi.org/10.1016/j.conbuildmat.2015.09.056.
[21] F. Ljunggren, C. Simmons, K. Hagberg, Correlation between sound insulation and occupants' perception – proposal of alternative single number rating of impact sound, Appl. Acoust. 85 (2014) 57–68, https://doi.org/10.1016/j.apacoust.2014.04.003.
[22] F. Ljunggren, C. Simmons, R. Öqvist, Correlation between sound insulation and occupants' perception – proposal of alternative single number rating of impact sound, part II, Appl. Acoust. 123 (2017) 143–151, https://doi.org/10.1016/j.apacoust.2017.03.014.
[23] F. Morandi, S. De Cesaris, M. Garai, L. Barbaresi, Measurement of flanking transmission for the characterisation and classification of cross laminated timber junctions, Appl. Acoust. 141 (2018) 213–222, https://doi.org/10.1016/j.apacoust.2018.07.009.
[24] EN ISO 10848-1:2017, Acoustics — Laboratory and Field Measurement of Flanking Transmission for Airborne, Impact and Building Service Equipment Sound between Adjoining Rooms — Part 1: Frame Document, 2017.
[25] A. Di Bella, L. Dall'Acqua d'Industria, M.R. Valluzzi, A. Pengo, L. Barbaresi, F. Di Nocco, F. Morandi, Flanking transmission in CLT buildings: comparison between vibration reduction index measurements for different mounting conditions, in: INTER-NOISE 2019 MADRID - 48th International Congress and Exhibition on Noise Control Engineering, 2019.
[26] F. Loriggiola, L. Dall'Acqua D'Industria, N. Granzotto, A. Di Bella, Acoustics behaviour of CLT structure: transmission loss, impact noise insulation and flanking transmission evaluations, in: Acoustics 2019, Sound Decisions: Moving Forward with Acoustics - Proceedings of the Annual Conference of the Australian Acoustical Society, 2020.
[27] Å. Bolmsvik, A. Brandt, Damping assessment of light wooden assembly with and without damping material, Eng. Struct. 49 (2013) 434–447, https://doi.org/10.1016/j.engstruct.2012.11.026.
[28] A. Speranza, L. Barbaresi, F. Morandi, Experimental analysis of flanking transmission of different connection systems for CLT panels, in: WCTE 2016 - World Conference on Timber Engineering, 2016.
[29] L. Barbaresi, F. Morandi, M. Garai, A. Speranza, Experimental measurements of flanking transmission in CLT structures, Proceedings of Meetings on Acoustics 28 (2016), https://doi.org/10.1121/2.0000433.

[30] D. Casagrande, S. Rossi, T. Sartori, R. Tomasi, Proposal of an analytical procedure and a simplified numerical model for elastic response of single-storey timber shear-walls, Construct. Build. Mater. 102 (2016) 1101–1112, https://doi.org/10.1016/j.conbuildmat.2014.12.114.
[31] EN 1995, Eurocode 5: Design of Timber Structures, Comité Européen de Normalisation, 2014.
[32] EN 338:2016, Structural Timber. Strength Classes, 2016.
[33] ETA-14/0349, Österreichisches Institut für Bautechnik - OiB Member of EOTA, 2014.
[34] EN 14374, Timber Structures. Structural Laminated Veneer Lumber. Requirements, 2004.
[35] Isolgomma. Technical Sheet of Sylpro AD, 2018.
[36] ETA-11/0030, Rotho Blaas Self-Tapping Screws and Threaded Rods, ETA-Denmark, 2016.
[37] M. Diaferio, D. Foti, N.I. Giannoccaro, Identification of the modal properties of a squat historic tower for the tuning of a FE model, in: 6th International Operational Modal Analysis Conference, IOMAC 2015, 2015.
[38] S. Ivorra, N.I. Giannoccaro, D. Foti, Simple model for predicting the vibration transmission of a squat masonry tower by base forced vibrations, Struct. Control Health Monit. 26 (2019) 1–21, https://doi.org/10.1002/stc.2360.
[39] Structural Vibration Solutions, ARTeMIS Modal, v. 6, 2019.
[40] E. Reynders, M. Schevenels, G. De Roeck, MACEC 3.3: A Matlab Toolbox for Experimental and Operational Modal Analysis, 2014.
[41] R.J. Allemang, D.L. Brown, A correlation coefficient for modal vector analysis, in: Proceedings of the 1st International Modal Analysis Conference, Orlando, 8-10 November 1982, 1982, pp. 110–116.
[42] ETA-11/0030, Rotho Blaas Self-Tapping Screws and Threaded Rods, ETA-Denmark, 2020.
[43] ETA-12/0063, Self-tapping screws for use in timber constructions, Österreichisches Institut für Bautechnik - OiB Member of EOTA, 2013.
[44] L. Franco, L. Pozza, A. Saetta, M. Savoia, D. Talledo, Strategies for structural modelling of CLT panels under cyclic loading conditions, Eng. Struct. 198 (2019), https://doi.org/10.1016/j.engstruct.2019.109476.
[45] F. Lorenzoni, M.R. Valluzzi, C. Modena, Seismic assessment and numerical modelling of the sarno baths, pompeii, J. Cult. Herit. 40 (2019) 288–298, https://doi.org/10.1016/j.culher.2019.04.017.
[46] A. Formisano, G. Di Lorenzo, L. Krstevska, R. Landolfo, Fem model calibration of experimental environmental vibration tests on two churches hit by L'aquila earthquake, Int. J. Architect. Herit. 15 (2021) 113–131, https://doi.org/10.1080/15583058.2020.1719233.
[47] C. Baggio, V. Sabbatini, S. Santini, C. Sebastiani, Comparison of different finite element model updates based on experimental onsite testing: the case study of San Giovanni in Macerata, Journal of Civil Structural Health Monitoring 11 (2021) 767–790, https://doi.org/10.1007/s13349-021-00480-1.
[48] F. Bianconi, G.P. Salachoris, F. Clementi, S. Lenci, A genetic algorithm procedure for the automatic updating of fem based on ambient vibration tests, Sensors 20 (2020) 1–17, https://doi.org/10.3390/s20113315.
[49] S. Cattari, S. Degli Abbati, S. Alfano, A. Brunelli, F. Lorenzoni, F. da Porto, Dynamic calibration and seismic validation of numerical models of URM buildings through permanent monitoring data, Earthq. Eng. Struct. Dynam. 50 (2021) 2690–2711, https://doi.org/10.1002/eqe.3467.
[50] J. Milosevic, S. Cattari, R. Bento, Definition of fragility curves through nonlinear static analyses: procedure and application to a mixed masonry-RC building stock, Bull. Earthq. Eng. 18 (2020) 513–545, https://doi.org/10.1007/s10518-019-00694-1.
[51] A. Sandoli, C. D'Ambra, C. Ceraldi, B. Calderoni, A. Prota, Role of perpendicular to grain compression properties on the seismic behaviour of CLT walls, J. Build. Eng. 34 (2021), https://doi.org/10.1016/j.jobe.2020.101889.
[52] A. Ringhofer, Stiffness Properties of Axially Loaded Self-Tapping Screws, COST Action FP1402 "Basis of Structural Timber Design" [COST-STSM-Fp1402-30283], 2015.
[53] R. Jockwer, A. Jorissen, Stiffness and deformation of connections with dowel-type fasteners, in: C. Sandhaas, J. Munch-Andersen, P. Dietsch (Eds.), Design of Connections in Timber Structures. A State-Of-The-Art Report by COST Action FP1402/WG3, 2018, pp. 95–126.
[54] N.M.M. Maia, J.M.M. Silvia, Theoretical and Experimental Modal Analysis, Research Studies Press, Taunton, 1997.
[55] T. Zordan, B. Briseghella, T. Liu, Finite element model updating of a tied-arch bridge using Douglas-Reid method and Rosenbrock optimization algorithm, J. Traffic Transport. Eng. 1 (2014) 280–292, https://doi.org/10.1016/S2095-7564(15)30273-7.
[56] L. Pozza, M. Savoia, L. Franco, A. Saetta, D. Talledo, Effect of different modelling approaches on the prediction of the seismic response of multi-storey CLT buildings, International Journal of Computational Methods and Experimental Measurements 5 (2017) 953–965, https://doi.org/10.2495/CMEM-V5-N6-953-965.
[57] M. Yasumura, K. Kobayashi, M. Okabe, T. Miyake, K. Matsumoto, Full-scale tests and numerical analysis of low-rise CLT structures under lateral loading, J. Struct. Eng. 142 (2016) 1–12, https://doi.org/10.1061/(ASCE)ST.1943-541X.0001348.
[58] H.J. Blass, P. Fellmoser, Design of solid wood panels with cross layers, in: Proceedings of the 8th World Conference on Timber Engineering 2004, 14-17 June, Lahti, Finland, 2004.
[59] M. Follesa, I.P. Christovasilis, D. Vassallo, M. Fragiacomo, A. Ceccotti, Seismic design of multi-storey cross laminated timber buildings according to eurocode 8, Progettazione sismica di edifici multipiano in cross laminated timber secondo l'Eurocodice 8, Ingegneria Sismica 30 (2013).
[60] M. Fragiacomo, B. Dujic, I. Sustersic, Elastic and ductile design of multi-storey crosslam massive wooden buildings under seismic actions, Eng. Struct. 33 (2011) 3043–3053, https://doi.org/10.1016/j.engstruct.2011.05.020.
[61] CNR - Consiglio Nazionale delle Ricerche, Istruzioni per la Progettazione, l'Esecuzione ed il Controllo di Strutture di legno, 2018.
[62] R. Crocetti, P.J. Gustafsson, U.A. Girhammar, L. Costa, A. Asimakidis, Nailed steel plate connections: strength and ductile failure modes, Structures (2016), https://doi.org/10.1016/j.istruc.2016.07.003.
[63] I. Gavric, A. Ceccotti, M. Fragiacomo, Experimental cyclic tests on cross-laminated timber panels and typical connections, in: XIV Convegno ANIDIS "L'Ingegneria Sismica in Italia, 2011. Bari, 18 - 22 Settembre 2011.
[64] I. Gavric, M. Fragiacomo, A. Ceccotti, Cyclic behaviour of typical metal connectors for cross-laminated (CLT) structures, Materials and Structures/Materiaux et Constructions 48 (2015) 1841–1857, https://doi.org/10.1617/s11527-014-0278-7.
[65] A.L.Y. Ng, H.H. Lau, K. Roy, G.M. Raftery, J.B.P. Lim, The behavior of cold-formed steel and Belian hardwood self-tapping screw connections, in: Proceedings of the Cold-Formed Steel Research Consortium Colloquium 17-19 October 2022, Cfsrc.Org), 2022.
[66] A.L.Y. Ng, H.H. Lau, Z. Fang, K. Roy, G.M. Raftery, J.B.P. Lim, Experimental studies of timber to cold-formed steel connections with self-drilling screws, Structures 49 (2023) 492–507, https://doi.org/10.1016/j.istruc.2023.01.111.
[67] J.M.W. Brownjohn, F. Magalhaes, E. Caetano, A. Cunha, Ambient vibration re-testing and operational modal analysis of the Humber Bridge, Eng. Struct. 32 (2010) 2003–2018, https://doi.org/10.1016/j.engstruct.2010.02.034.
[68] W. de A. Thomaz, D.Y. Miyaji, E. Possan, Comparative study of dynamic and static Young's modulus of concrete containing basaltic aggregates, Case Stud. Constr. Mater. 15 (2021), https://doi.org/10.1016/j.cscm.2021.e00645.
[69] A. Ceccotti, M. Lauriola, M. Pinna, C. Sandhaas, SOFIE Project - cyclic tests on cross-laminated wooden panels, in: 9th World Conference on Timber Engineering 2006 (WCTE 2006), Portland, Oregon, USA 6-10 August 2006, 2006.
[70] A. Ceccotti, M. Follesa, C. Sandhaas, Sofie project – test results on the lateral resistance of cross-laminated wooden panels, in: First European Conference on Earthquake Engineering and Seismology, Geneva, Switzerland, 3-8 September 2006, 2006.